Neuroscience Letters 513 (2012) 141–145

Contents lists available at SciVerse ScienceDirect

Neuroscience Letters

journal homepage: www.elsevier.com/locate/neulet

ISOMAP induced manifold embedding and its application to Alzheimer's disease and mild cognitive impairment

Hyunjin Park*, the ADNI[1]

Department of Biomedical Engineering, Gachon University, Republic of Korea

ARTICLE INFO

Article history:
Received 30 September 2011
Received in revised form 6 February 2012
Accepted 7 February 2012

Keywords:
Manifold embedding
ISOMAP
Alzheimer's disease
Mild cognitive impairment
Shape quantification
Morphometry

ABSTRACT

Neuroimaging data are high dimensional and thus cumbersome to analyze. Manifold learning is a technique to find a low dimensional representation for high dimensional data. With manifold learning, data analysis becomes more tractable in the low dimensional space. We propose a novel shape quantification method based on a manifold learning method, ISOMAP, for brain MRI. Existing work applied another manifold learning method, multidimensional scaling (MDS), to quantify shape information for distinguishing Alzheimer's disease (AD) from normal. We enhance the existing methodology by (1) applying it to distinguish mild cognitive impairment (MCI) from normal, (2) adopting a more advanced manifold learning technique, ISOMAP, and (3) showing the effectiveness of the induced low dimensional embedding space to predict key clinical variables such as mini mental state exam scores and clinical diagnosis using the standard multiple linear regression. Our methodology was tested using 25 normal, 25 AD, and 25 MCI patients.

Introduction

Many neurodegenerative diseases cause unique morphological changes in brain anatomy. Only certain structures of the brain are selectively affected by the diseases, while the rest of the brain remains the same. Alzheimer's disease (AD) is known to cause atrophy in the hippocampus region. Computational anatomy (CA) is a research field which applies a computer algorithm to quantify such changes in shape information [8]. The task of measuring shape is not simple and has been a matter of significant controversy [2,4]. There are two main approaches for measuring shape. The first approach, deformation based morphometry (DBM), assumes that all shape information is encoded in the deformation fields, which relates one brain scan with another scan [3]. The second approach, voxel based morphometry (VBM), assumes that all shape information is encoded in some scalar function of the registered scans [1]. Two scans are segmented and then linearly registered so that both scans are in the same spatial coordinates in the VBM approach. Shape information is assessed by voxel-wise difference in the labels after registration. DBM uses deformation fields obtained from registrations of a population and identifies differences in the relative positions of structures within the region of interest (ROI). One major weakness of DBM is that it requires a very accurate registration algorithm for computation of the displacement field. We adopt the DBM approach and assume all the necessary shape information is given by the displacement fields. This study focuses on AD and mild cognitive impairment (MCI). Many patients with MCI often convert to AD later in the disease progression. MCI has been extensively studied as detection of MCI is highly related to early diagnosis of AD. We apply a computer algorithm to measure shape differences so that AD or MCI patients may be distinguished from normal patients. The shape information is computed from the displacement field and the displacement field is burdened with high dimensionality. The dimension of a displacement field is as high as the number of voxels of the given scan, which may number in the millions. Many displacement fields must be considered when studying a population. Hence, the dimension of the overall data is quite large. One way to ease the burden of high dimensionality is to apply manifold learning techniques. Manifold learning is a technique used for finding a low dimensional representation for high dimensional data [10]. Researchers applied manifold learning methods to neuroimaging data in order to effectively represent shape information in a low dimensional embedding space [7].

Park et al. [12] applied multidimensional scaling (MDS) combined with bending energy of the displacement field to discriminate shape information between AD from normal controls [12]. Their approach reported effective separation of AD from normal controls and showed robustness to errors in displacement fields improving the major weakness with DBM based shape quantification. We

* Tel.: +82 32 820 4432; fax: +82 32 820 4059.
E-mail address: hyunjinp@gachon.ac.kr

[1] Data used in the preparation of this article were obtained from the Alzheimer's Disease Neuroimaging Initiative (ADNI) database (www.loni.ucla.edu/ADNI).

0304-3940/$ – see front matter © 2012 Elsevier Ireland Ltd. All rights reserved.
doi:10.1016/j.neulet.2012.02.016

extended Park et al. [12] to include MCI patients in this study. Here we adopted a more advanced manifold learning technique called ISOMAP instead of MDS. Shape information lies with non-Euclidean Riemannian space and the induced distance is known to be geodesic. ISOMAP better represents geodesic distances and hence is better suited for studying shape information. In the previous study, the induced low dimensional embedding space was used as a feature space for a kNN classifier to distinguish between AD and normal. We used the low dimensional embedding space as a feature space to perform classical statistical tests for clinical variables, including score of mini mental state exam (MMSE) and clinical diagnosis. Using multiple linear regression, we performed statistical testing in order to determine how well the low dimensional embedding space was able to predict MMSE score and clinical diagnosis. Support vector machine (SVM) classifier combined with advanced feature selection has been successfully applied to classify normal and AD for PET, resulting up to 90% classification accuracy [11]. The SVM based method is one of the state of the art methods for classifying AD and normal. We compared the performance of the method in this study with that of SVM based method in the results section. In summary, this study builds on the work of Park et al. [12] and we extended the methodology by (1) testing its applicability to MCI patients, (2) adopting a more advanced manifold learning technique, and (3) testing the effectiveness of the low dimensional embedding space as a platform to carry out statistical tests for key clinical variables.

Materials and methods

Our shape quantification methodology is very similar to the previous work [12]. Here we briefly describe the overall framework emphasizing the differences.

Registration framework

Registration is a task of finding the geometric mapping between two images, so that one image can be mapped onto the other. This study used mutual information (MI) as the similarity measure and thin-plate splines (TPS) as the geometric interpolant [9]. There are many definitions of MI and we adopt the metric MI in the equation below.

$$\mathrm{MI}(X, Y) = H(X|Y) + H(Y|X) \tag{1}$$

where X is the intensity distribution of scan X, Y is the intensity distribution of scan Y, $H(X|Y)$ is the conditional entropy of X given Y, and $H(Y|X)$ is the conditional entropy of Y given X. This particular variant of MI satisfies the metric property including symmetry and triangular inequality. Many manifold learning techniques work best with metric distance measures.

Distance measure

Registration between two scans yields a geometric transform optimized for maximization of a certain cost function. The displacement field is a collection of evaluations of the geometric transform at all voxel locations. The entire deformation field, whose order is equal to the number of voxels, is compressed to a single scalar value. The scalar value is the geometric distance, hereafter called distance, which measures the roughness of the geometric transform that associates the coordinate spaces of two scans. If the geometric transform is complex between two images, then the distance measure will be high. If the geometric transform is simple, then the distance measure will be small. We adopted the integral of the squared value of the second-order derivative of the geometric transform as the distance measure. We chose the second-order derivative in order to ensure invariance to affine transforms. The formulation for the distance measure is given below.

$$d^2 = \iint \left(\frac{\partial^2 f_x}{\partial x^2}\right)^2 + 2\left(\frac{\partial^2 f_x}{\partial x \partial y}\right)^2 + \left(\frac{\partial^2 f_x}{\partial y^2}\right)^2 dxdy + \iint \left(\frac{\partial^2 f_y}{\partial x^2}\right)^2 + 2\left(\frac{\partial^2 f_y}{\partial x \partial y}\right)^2 + \left(\frac{\partial^2 f_y}{\partial y^2}\right)^2 dxdy \tag{2}$$

where f_x displacement in x and f_y displacement in y.

Formulation in (2) is for 2D and can be easily extended for 3D. This distance is called the bending energy. The proposed distance measure is based on the displacement field. Others adopted a distance measure based on grayscale information of the registered scans [14]. If two scans can be registered with a high MI value, it is likely that two scans are similar hence the distance between the two should be small. Thus, the inverse of MI (i.e., 1/MI) may be used as a distance measure. We compared our distance measure based on the displacement field (i.e., bending energy) with the distance measure based on grayscale values (i.e., metric MI) in the results section.

ISOMAP

ISOMAP is a manifold learning technique based on pair-wise distances derived from high dimensional data [13]. Compared to traditional manifold learning methods such as MDS, it approximates the geodesic distances using weighted neighborhood graphs. Shape information occupies non-Euclidean Riemannian space and the induced distance is geodesic, thus ISOMAP is well equipped to deal with shape information. Given a set of distances in the distance matrix D, ISOMAP outputs a set of coordinates in a user-specified dimension. The dimension of ISOMAP output is determined based on the eigenstructure of the distance matrix. The output coordinates are in the standard Euclidean space of the user-chosen dimension. ISOMAP considers only distance measures from nearby objects and approximates large distances from distant objects by composition of small scale distances. It basically trusts only small distance values and approximates the large distance values using composition of small distances. For scans that are relatively similar and thus easy to register, the resulting bending energy is likely to be small and ISOMAP places high confidence on such distances. For scans that are vastly different and thus difficult to register, the resulting bending energy is likely to be large and ISOMAP does not trust such large bending energy values. Instead, ISOMAP approximates the difficult registration between two vastly different scans by composition of small scale and easy to do registration tasks.

Framework for shape quantification

ISOMAP produces relative positional locations from a collection of pair-wise distances, which in turn assigns a low dimensional coordinate for each MRI scan. The key idea is to use a distance measure that quantifies distances between MRI scans. We adopted a distance measure called bending energy, which is based on the displacement field. Output of ISOMAP is often visualized on a scatter plot, where each dot represents a scan. In the scatter plot, the relative positions of all scans are plotted in the Euclidean space of a user-chosen dimension. We hypothesize that scans of the same type will be placed adjacent and scans of different types will be placed separately. Therefore, we expect a scatter plot in which two distinct clusters can be observed. The low dimensional embedding space (i.e., ISOMAP output coordinates) may be used as a feature space for quantification of shape information. In this study, the ISOMAP embedding space was used as the feature space for

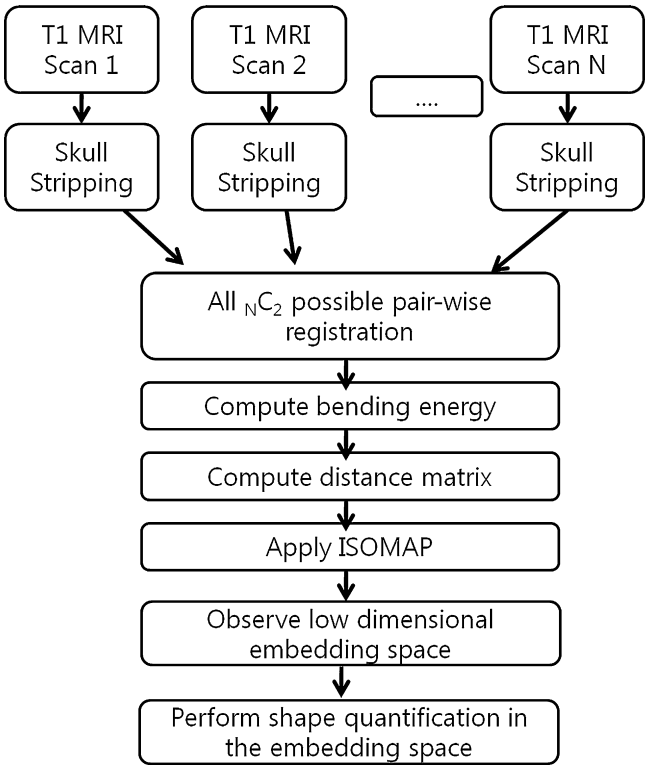

Fig. 1. Shape quantification procedures using ISOMAP for N scans.

(1) automatic classification of diagnostic groups, and (2) for performing multiple linear regression for MMSE scores and clinical diagnosis. Fig. 1 shows the shape quantification procedure for N scans.

Data acquisition

We obtained MRI image data and MMSE scores from the ADNI database. Data used in the preparation of this study were obtained from the ADNI database (www.loni.ucla.edu/ADNI). We acquired 75 MRI brain scans and noted the MMSE score for each patient. 25 AD scans aged between 66 and 82 and consisted of 12 males and 13 females. 25 MCI scans aged between 60 and 90 and consisted of 14 males and 11 females. 25 normal scans aged between 71 and 90 and consisted of 14 males and 11 females. All MRIs were sagittal T1-weighted scans and had typical dimensions of $256 \times 256 \times 166$ and resolutions of $0.94\,\text{mm} \times 0.94\,\text{mm} \times 1.2\,\text{mm}$. The scans were collected using a 1.5 T GE Signa scanner with an MR-RAGE acquisition sequence.

Data pre-processing

Non-brain tissue sections were removed using a procedure similar to "skull stripping". We implemented our own algorithm based on registration. First, registration between the labeled International Consortium for Brain Mapping (ICBM) scan and the user-chosen scan was established. Second, labels from the ICBM scan were carried onto the user scan and then used as a mask. Masked voxels contained only brain tissues, including white matter, gray matter, and cerebral spinal fluid (CSF). With this mask, the user-chosen scan could be stripped of non-brain tissues. After removal of all scans of non-brain tissues, pair-wise registrations using 50 control points were performed. The 50 control points were distributed almost uniformly over the entire brain.

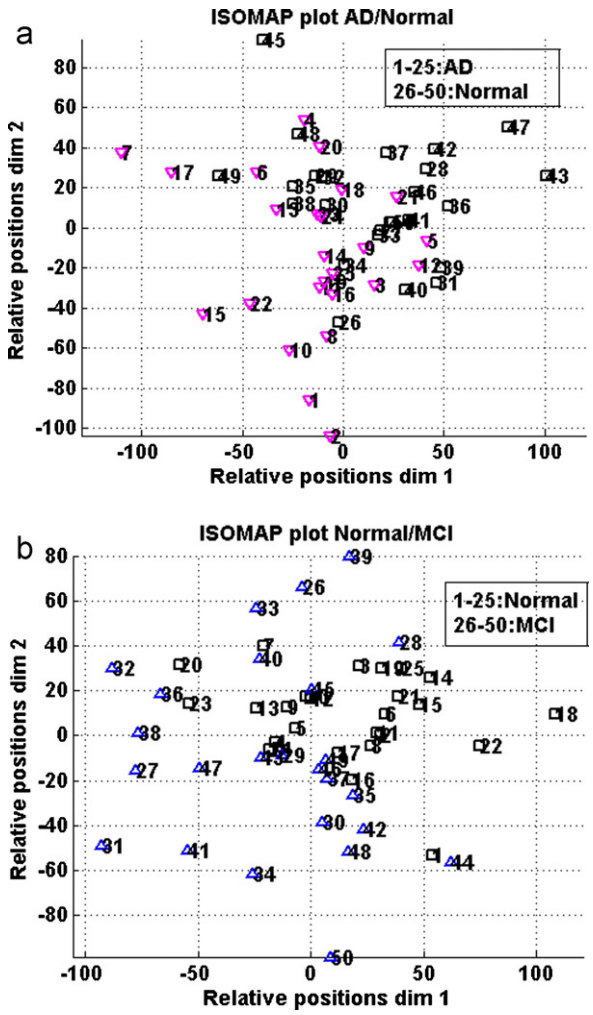

Fig. 2. Output of ISOMAP. The top figure shows separability between AD and normal, while the bottom figure shows separability between MCI and normal. Major separation occurred along the first dimension (horizontal axis) for AD/Normal and MCI/Normal. The figures show the first two dimensions out of the three-dimensional ISOMAP coordinates.

Experimental setup

ISOMAP based shape quantification was applied to the following three scenarios where each contained two groups for comparison: (1) normal control and AD, (2) normal control and MCI, and (3) AD and MCI. For each scenario, there were 50 brain MRI scans involved; thus, a total of 50 choose 2 (i.e., 1225) pair-wise registrations were performed and the resulting bending energies were entered into the 50×50 distance matrix. Once the distance matrix was computed, ISOMAP was applied with 29 nearest neighbor setting and the results were analyzed in three dimensions. The dimension of ISOMAP was chosen based on the eigenvalues of the distance matrix. We chose the number L as the dimension, such that after L largest eigenvalues, the next occurring eigenvalue dropped dramatically.

Results

Separability between clusters

Fig. 2 shows a scatter plot of ISOMAP output for distinguishing (1) normal control and AD (Fig. 2a), and (2) normal control and MCI (Fig. 2b). Both scenarios showed clear separation between clusters

Table 1
p-Values for separation of clusters using different distance measures.

Clusters being compared	Distance measure	
	Bending energy	Metric MI
AD/Normal	0.003	0.538
MCI/Normal	0.006	0.362
AD/MCI	0.161	0.625

being compared. For separation of AD and normal, the separation was evident along the horizontal dimension and for separation of MCI and normal, the separation was also observed along the horizontal dimension. To quantify separability between clusters being compared, a two-sample *T*-test was applied to the first coordinate dimension (i.e., horizontal dimension). The *p*-value of AD/Normal was small, which showed that AD and normal control can be easily distinguished. The *p*-value of MCI/Normal was still small (i.e., $0.006 < 0.05$), but was larger than the case of AD/Normal, which showed that MCI and normal can be distinguished at the 0.05 level; however, they were not as easily distinguishable as the AD/Normal case. The *p*-value of MCI/AD was large; thus, they were not distinguishable at the 0.05 level.

Comparison of bending energy and MI as the distance measure

We compared the performance of ISOMAP based shape quantification using bending energy as the distance measure with that of metric MI as the distance measure. *p*-Values of two-sample *T*-tests to quantify the separability between clusters being were compared in Table 1. The *p*-values of all three scenarios using metric MI as the distance measure were larger than those using bending energy and all were greater than 0.05. Using metric MI as the distance measure did not provide enough sensitivity to distinguish the following three comparison groups, AD/Normal, MCI/Normal, and AD/MCI. MI is computed from a joint grayscale distribution of registered scans. Spatial information is removed when the joint distribution is computed. Loss of spatial information during the construction of the joint distribution may negatively affect the sensitivity of metric MI as the distance measure.

Classification using a kNN classifier

Here we used the embedding space as a feature space for automatic classification. We applied a well-known k-nearest neighbor (kNN) classifier, where k was set to three. A leave-one-out approach was adopted when computing the classification performance. For each case being tested, we trained the classifier using the remaining 49 cases and then computed the classification performance for the test case. The process was repeated for all 50 MRI scans of each scenario and the classification rate is reported in Table 2. For comparison, we implemented a classification algorithm based on hippocampus volume. AD and MCI patients were reported to have a smaller hippocampus, compared with the normal control; thus, hippocampus volume has been used as a feature of a classifier in order to distinguish AD/Normal and MCI/Normal [6]. Since manual segmentation of the hippocampus for 75 scans would be very laborious, we used the well-known FSL software to achieve automatic segmentation of the hippocampus and computed its volume. We used the same kNN classifier and leave-one-out approach; the classification rate is reported in Table 2. From Table 2, classification rates were better with our ISOMAP embedding based kNN classifier for differentiation of AD/Normal and MCI/Normal groups, compared to the hippocampus volume based classifier. For differentiation of AD/MCI, neither was very good, as both were barely better than randomly flipping a coin (i.e., 50%). Existing automatic classification studies [5] tested on the same ADNI database reported a classification rate of 76% for distinguishing AD/Normal and 71% for distinguishing MCI/Normal; thus, our results showed better performance compared to existing research.

Table 2
Classification rates of various classifiers.

Classifier type	Clusters		
	AD/Normal	MCI/Normal	AD/MCI
kNN ($k = 3$) using ISOMAP embedding	84%	76%	56%
kNN ($k = 3$) using Hippocampus volume	76%	60%	54%
SVM using a linear kernel with dimensionality reduced features	76%	75%	70%

Comparison with an SVM classifier

The performance of the proposed kNN classifier was compared to that of the state of the art SVM based classifier in Table 2 [11]. The same leave-one-out approach was adopted. For the SVM based method, the high dimensionality of the observed features was reduced using principal component analysis (PCA) and linear discriminant analysis (LDA). The reduced features were then fed into the SVM classifier using a linear kernel. We applied the algorithm of [11] to a set of anatomical MRI instead of PET. This is because the focus of this paper is to see if we can distinguish AD/MCI from normal patients based on the feature space induced by a manifold learning method using only anatomical MRI. For classifying AD and normal, our method fared better. For classifying MCI and normal, both methods reported similar performance. For classifying AD and MCI, SVM based method was better. The proposed method performed equally or better than the SVM based method for two cases out of the three. The proposed method is based on a simple kNN classifier, if combined with an advanced classifier including SVM, it has an excellent potential to perform better and we leave this as future work. The focus of this paper is to show the usefulness of the induced space and we believe using a simple kNN classifier serves such purpose. The proposed method follows the assumptions of DBM, while the SVM based method follows the assumption of VBM as the features were obtained from voxel values in the SVM based method. For researchers not subscribing to VBM assumptions, the proposed method can be a useful alternative to classify between AD and normal with "on par" performance compared to the state of the art SVM based methods.

Low dimensional embedding space and statistical tests

In neuroimaging analysis, the most commonly performed statistical test is the comparison of two groups using a simple *T*-test. A simple *T*-test compares one-dimensional observations, while ISOMAP embedding space could be multi-dimensional (e.g., three dimensional coordinates). Note that dimensionality of embedding space is typically small (e.g., typically lower than five). Multiple linear regression is a framework for full incorporation of multi-dimensionality of the embedding space. Using multiple linear regression, we tested how well the low dimensional embedding space of ISOMAP (i.e., coordinates in the scatter plot) was able to predict MMSE score and clinical diagnosis for the three scenarios (Table 3). If AD/Normal groups were considered, both MMSE scores and diagnosis could be well predicted by linear regression witnessed by large *F*-statistics and low *p*-value. The statistical strength weakened when the MCI/Normal group was considered, as *F*-statistics decreased and *p*-value increased. Neither MMSE score nor diagnosis could be meaningfully predicted from the MCI/AD

Table 3
Multiple linear regression models for MMSE and diagnosis ($\varepsilon = 10^{-8}$).

Clinical variable	Groups being compared	R^2 statistics	F-Statistics	p-Value
MMSE scores	AD/Normal	0.465	13.306	$<\varepsilon$
	MCI/Normal	0.056	0.906	0.446
	AD/MCI	0.046	0.740	0.533
Diagnosis (AD/MCI/Normal)	AD/Normal	0.546	18.437	$<\varepsilon$
	MCI/Normal	0.222	4.381	0.009
	AD/MCI	0.092	1.547	0.215

group. The most separable group (i.e., AD/Normal) would have the maximum statistical power to predict clinical variables, while the least separable group (i.e., AD/MCI) would be least able to predict the clinical variables. Compared with the recent study [7], use of our method resulted in similar performance in terms of F-statistics and p-value.

Discussion

Neuroimaging data are almost always high dimensional and application of statistical tests on high dimensional data is prone to noise. Applying manifold learning results in a low dimensional embedding space to analyze shape information. Statistical test results performed in a low dimensional space are more robust than those performed in a high dimensional space due to the reduced dimensionality. The clinically important issue is early detection of AD. A patient might undergo an MRI scan every 6 months, and we would like to predict the onset of AD before the actual conversion from normal to AD occurs. This scenario will lead to time-series analysis. We described a framework for quantification of group-wise differences and we did not consider time series data in this study. The same ISOMAP induced low dimensional space may still serve as a good platform for time-series analysis and we leave this important problem as future work.

Acknowledgements

This study was supported by the Basic Science Research Program through the National Research Foundation of Korea grant 20100023233. Data collection and sharing for this project was funded by the ADNI (NIH U01 AG024904).

References

[1] J. Ashburner, K.J. Friston, Voxel-based morphometry – the methods, Neuroimage 11 (2000) 805–821.
[2] J. Ashburner, K.J. Friston, Why voxel-based morphometry should be used, Neuroimage 14 (2001) 1238–1243.
[3] J. Ashburner, C. Hutton, R.S.J. Frackowiak, I. Johnsrude, C. Price, K.J. Friston, Identifying global anatomical differences: deformation-based morphometry, Hum. Brain Mapp. 6 (1998) 348–357.
[4] F.L. Bookstein, Voxel-based morphometry should not be used with imperfectly registered images, Neuroimage 14 (2001) 1454–1462.
[5] M. Chupin, E. Geradin, R. Cuingnet, C. Boutet, L. Lemieux, S. Lehericy, H. Benali, L. Gaenero, O. Colliot, ADNI, Fully automatic hippocampus segmentation and classification in Alzheimer's disease and mild cognitive impairment applied on data from ADNI, Hippocampus 19 (2009) 579–587.
[6] S. Duchesne, A. Caroli, C. Geroldi, C. Barillot, G.B. Frisoni, D.L. Collins, MRI-based automated computer classification of probable AD versus normal controls, IEEE Trans. Med. Imaging 27 (2008) 509–520.
[7] S. Gerber, T. Tasdizen, P.T. Fletcher, S. Joshi, R. Whitaker, ADNI, Manifold modeling for brain population analysis, Med. Image Anal. 14 (2010) 643–653.
[8] U. Grenander, M.I. Miller, Computational anatomy, Q. Appl. Math. 4 (1998) 617–694.
[9] D.L.G. Hill, P.G. Batchelor, M. Holden, D.J. Hawkes, Medical image registration, Phys. Med. Biol. 46 (2001) r1–r45.
[10] J.A. Lee, M. Verleysen, Nonlinear Dimensionality Reduction, Springer, 2007.
[11] M. López, J. Ramírez, J.M. Górriz, I. Álvarez, D. Salas-Gonzalez, F. Segovia, R. Chaves, P. Padilla, M. Gómez-Río, ADNI, Principal component analysis-based techniques and supervised classification schemes for the early detection of Alzheimer's disease, Neurocomputing 74 (2011) 1260–1271.
[12] H. Park, J. Seo, ADNI, Application of multidimensional scaling to quantify shape in Alzheimer's disease and its correlation with mini mental state examination: a feasibility study, J. Neurosci. Methods 194 (2011) 380–385.
[13] S.T. Roweis, L.K. Saul, Nonlinear dimensionality reduction by locally linear embedding, Science 290 (2000) 2323–2326.
[14] R. Wolz, P. Aljabar, J.V. Hajnal, A. Hammers, D. Ruckert, LEAP, ADNI, Learning embedding for atlas propogation, Med. Image Anal. 49 (2010) 1316–1325.